Cell Research

ARTICLE

Poly(ADP-ribose) mediates asymmetric division of mouse oocyte

Bingteng Xie[1,2], Lu Zhang[1,2], Huiling Zhao[3], Qingyun Bai[3], Yong Fan[4], Xiaohui Zhu[1], Yang Yu[1], Rong Li[1], Xin Liang[5], Qing-Yuan Sun[6], Mo Li[1,2] and Jie Qiao[1,2]

Before fertilization, mammalian oocyte undergoes an asymmetric division which depends on eccentric positioning of the spindle at the oocyte cortex to form a polar body and an egg. Since the centriole is absent and, as a result, the polar array microtubules are not fully developed in oocytes, microtubules have seldom been considered as required for eccentric positioning of the spindle, while actin-related forces have instead been proposed to be primarily responsible for this process. However, the existing models are largely conflicting and the underlying mechanism of asymmetric division is still elusive. Here we show that poly(ADP-ribose) (PAR) is enriched at mouse oocyte cortical area throughout meiosis. Specific removal of cortical PAR results in an ectopic spindle and a failure of asymmetric division. During spindle migration, when the spindle deviates from the center of oocyte by a pushing force of cytoplasmic actin, the short polar array microtubules emanating from the juxtacortical spindle pole extend to the cortex and penetrate into cortical PAR, docking and stabilizing the spindle at the cortex which facilitates the asymmetric division. This process depends on the affinity between PAR and microtubule-associated proteins such as Spindly, which contributes to a physical link for cortical PAR and the spindle. Notably, fusing a PAR-binding domain to end-binding protein 3, a plus-end tracking protein at the polar array microtubules, restores the asymmetric division of oocytes with Spindly knockdown. Thus, our work demonstrates a comprehensive mechanism for oocyte spindle positioning and asymmetric division.

Cell Research (2018) 28:462–475; https://doi.org/10.1038/s41422-018-0009-7

INTRODUCTION

For the early embryonic development, an oocyte retains most maternal stores during meiosis by extruding a small polar body before fertilization.[1,2] This asymmetric division depends on the migration of microtubule spindle to the oocyte cortex.[3–5] In mammals, oocytes in ovarian follicles are arrested at the diplotene stage of the first meiotic prophase, namely the germinal vesicle (GV) stage, until stimulated by the pituitary hormone surge.[6,7] When the meiotic process restarts, GV breakdown (GVBD) occurs accompanied by the spindle assembly.[8,9] The spindle starts the assembly process at the pericenter of oocyte, followed by the capture of the condensed chromosomes. At the end of the metaphase of the first meiosis (MI), the spindle carrying the chromosomes migrates to the cortex so that the oocyte can achieve asymmetric division. During the second meiosis, the spindle inherits the position from the first meiosis and maintains the asymmetric feature.[10,11] Errors in spindle positioning result in failure of asymmetric division and abnormalities in embryonic development. Thus, spindle positioning must be properly regulated in oocytes.

Over the past years, it is generally thought that the main force for spindle eccentric positioning in mammalian oocytes does not seem to rely on spindle microtubules per se due to the absence of the centriole and the resulting non-developed polar array microtubules (similar to astral microtubules in mitotic cells).[12,13] Unlike the well-developed astral microtubules and the small cell volume of mitotic cell, the short polar array microtubules emanating from spindle poles in oocyte cannot reach to the cortex.[14] Instead, most previous studies have focused on actin and indicated that actin regulates spindle movement in oocyte meiosis.[4,5,15–17] However, these studies lead to conflicting models and a unified theory has not been established. For example, some studies suggested that a cytoplasmic force formed by cytoplasmic actin around the spindle pushes the spindle toward the cortex,[15,18] while other work indicated that a short-haul actin force between the cortex and spindle pole pulls the spindle apparatus to the cortex, as evidenced by a dense actin signal connecting the spindle pole and the cortex.[5] Nevertheless, few studies considered the potential participation of spindle microtubules per se. Furthermore, the molecular mechanism responsible for clinching and stabilizing the spindle beneath the cortex remains unclear.

In this study, we find that poly(ADP-ribose) (PAR), a polymer of ADP-ribose, is significantly enriched at mouse oocyte cortex. This is very different from somatic cells where PAR is almost, if not all, restricted to the nucleus.[19] PAR, a polymer identified over half a

[1]Center for Reproductive Medicine, Peking University Third Hospital, 100191 Beijing, China; [2]Key Laboratory of Assisted Reproduction, Ministry of Education, 100191 Beijing, China; [3]School of Basic Medical Sciences, Peking University Health Science Center, 100191 Beijing, China; [4]Key Laboratory for Major Obstetric Diseases of Guangdong Province The Third Affiliated Hospital of Guangzhou Medical University, 510150 Guangzhou, China; [5]Tsinghua-Peking Center for Life Sciences, School of Life Sciences, Tsinghua University, 100084 Beijing, China and [6]State Key Laboratory of Stem Cell and Reproductive Biology, Institute of Zoology, Chinese Academy of Sciences, 100101 Beijing, China
Correspondence: Mo Li (limo@hsc.pku.edu.cn) or Jie Qiao (jie.qiao@263.net)
Bingteng Xie and Lu Zhang contributed equally to this work.

Received: 2 July 2017 Revised: 30 October 2017 Accepted: 5 January 2018
Published online: 20 February 2018

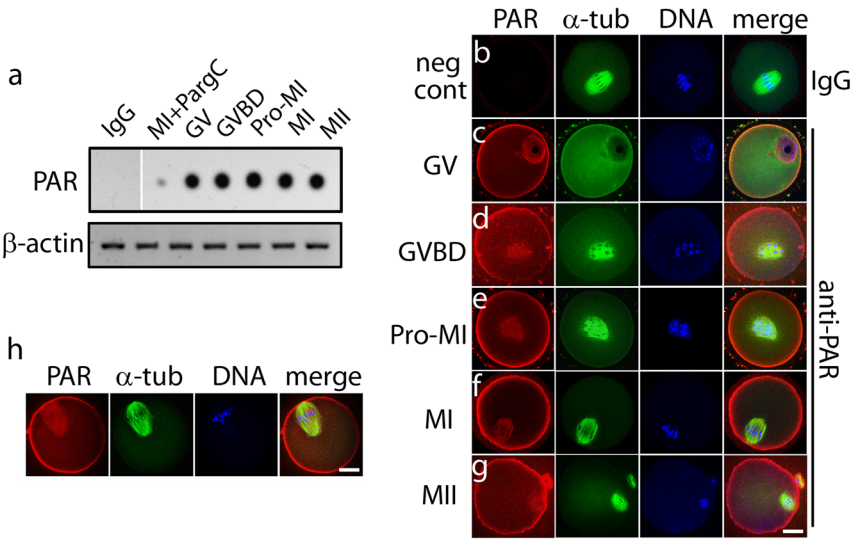

Fig. 1 PAR is enriched at cortex during mouse oocyte meiosis. **a** The content of PAR in different stages of oocyte meiosis. A total of 300 oocytes at each stage were harvested and lysed. The lysate was split for dot blot of PAR and western blot of β-actin, respectively. In dot blot, the lysate was dropped on nitrocellulose membrane followed by the immunoblot with PAR antibody. β-Actin was used as the loading control. Two negative controls were included, that is, IgG (lane 1), and MI oocyte lysate incubated with the purified Parg catalytic domain (PargC) in which PAR was mostly hydrolyzed (lane 2). **b–g** Subcellular localization of PAR during oocyte meiosis. Oocytes at each meiotic stage were harvested for immunofluorescent staining of PAR, microtubules, and DNA. Replacing of PAR antibody with IgG was used as a negative control. **h** Immunofluorescence of oocyte without zona pellucida. Scale bar, 20 μm

century ago, is synthesized by the PAR polymerases (PARPs) using NAD as a substrate.[20,21] For decades, PAR is believed to function primarily upon cellular stress such as DNA damage.[19,22,23] Here, we investigate the role of PAR in mouse oocyte meiosis. Specific removal of cortical PAR by "spindle exchanging" or targeting the catalytic domain of PAR glycohydrolase (Parg), a hydrolase that specifically degrades PAR[24,25] at oocyte cortex leads to a failure of asymmetric division. During its migration, the spindle can easily deviate from the center of the oocyte by a pushing force of cytoplasmic actin. When one pole of the spindle approaches oocyte cortex, short polar array microtubules emanating from this pole therefore catch cortical PAR, docking and stabilizing the spindle at the cortex which facilitates the asymmetric division of the oocyte. This process depends on a high affinity between PAR and microtubule-associated proteins such as Spindly, which contributes to a physical link for cortical PAR and the spindle. In oocytes with Spindly knocked down, fusing a PAR-binding domain to end-binding protein 3 (EB3), a plus-end hub at the polar array microtubules rescues the abnormally positioned spindle and the failure of asymmetric division. Thus, our work uncovers an undefined role of PAR and provides a comprehensive model for oocyte asymmetric division.

RESULTS

PAR is enriched in oocyte cortex during meiosis

To study the function of PAR in mouse oocyte asymmetric division, we examined PAR content during meiosis. Oocytes at different stages were harvested followed by dot blots of PAR, a method for detecting PAR that is highly branched and negatively charged.[23,26] To confirm the specificity of the antibody of PAR, two negative control groups were included. In one group, the PAR antibody was replaced with immunoglobulin G (IgG). In the other group, the cell lysate was treated by the purified catalytic domain of Parg (PargC), a glycohydrolase that specifically hydrolyzes PAR.[24,25] As shown in Fig. 1a, PAR was present in all stages of meiosis including GV, GVBD, prometaphase (pro-MI), MI, and metaphase of the second meiosis (MII) stages. We further examined the subcellular localization of PAR in oocytes. PAR existed in the nucleus in GV oocytes and associated with the spindle after GVBD (Fig. 1c–g; Fig. 1b showed the negative control in which IgG was used instead of PAR antibody). These observations are consistent with previous reports in somatic cells and frog egg extract.[27,28] Of note, PAR was intensely localized at the cortical area of the oocytes throughout the whole-meiotic maturation (Fig. 1c–g). To exclude the possibility of non-specific staining of the cortex, the sticky zona pellucida was removed from the oocyte before performing the immunofluorescence assay. We found that PAR was still present in the cortical area without zona pellucida (Fig. 1h). Moreover, another anti-PAR antibody purchased from a different manufacturer was used to repeat these experiments and PAR could still be observed in the cortex (Supplementary information, Figure S1A). Next we asked whether the cortical localization of PAR is a general phenotype for other cell types. Several somatic cell lines including 293T, NIH-3T3, primary mouse embryonic fibroblasts, MRC5 (human fetal lung fibroblasts), and MCF10A, a non-tumorigenic epithelial cell line derived from human breast, were subjected to immunofluorescent staining with PAR antibody. MCF10A cells treated by H_2O_2, a DNA-damaging agent,[29] were used as a positive control for PAR staining. Interestingly, little PAR staining could be found at the cortex of those cells (Supplementary information, Figure S1B), indicating that the cortical localization of PAR is unique to the mammalian oocytes compared to somatic cells, at least in the above-tested cells. The enrichment of PAR at the cortex likely suggests a unique function of PAR in the female germ cell.

Cortical PAR is required for spindle positioning to oocyte cortex

To gain insight into the role of cortical PAR, we inhibited the synthesis of PAR by knocking down mouse Parp family (Parp1 to Parp16) using a pool of Parp RNA interference (RNAi). The mRNA levels of all Parps were significantly reduced, as examined by quantitative PCR (Supplementary information, Figure S2A). Dot blot of PAR from lysed oocytes confirmed the effective depletion of the polymer (Fig. 2a). Upon Parp RNAi, the most significant phenotype was the intensely impaired spindle (Supplementary information, Figure S2B and C). This is not surprising given that PAR was localized at spindle and was required for spindle structure maintenance in Xenopus egg extract and somatic cells.[27,28] To distinguish the differential roles of PAR at the spindle

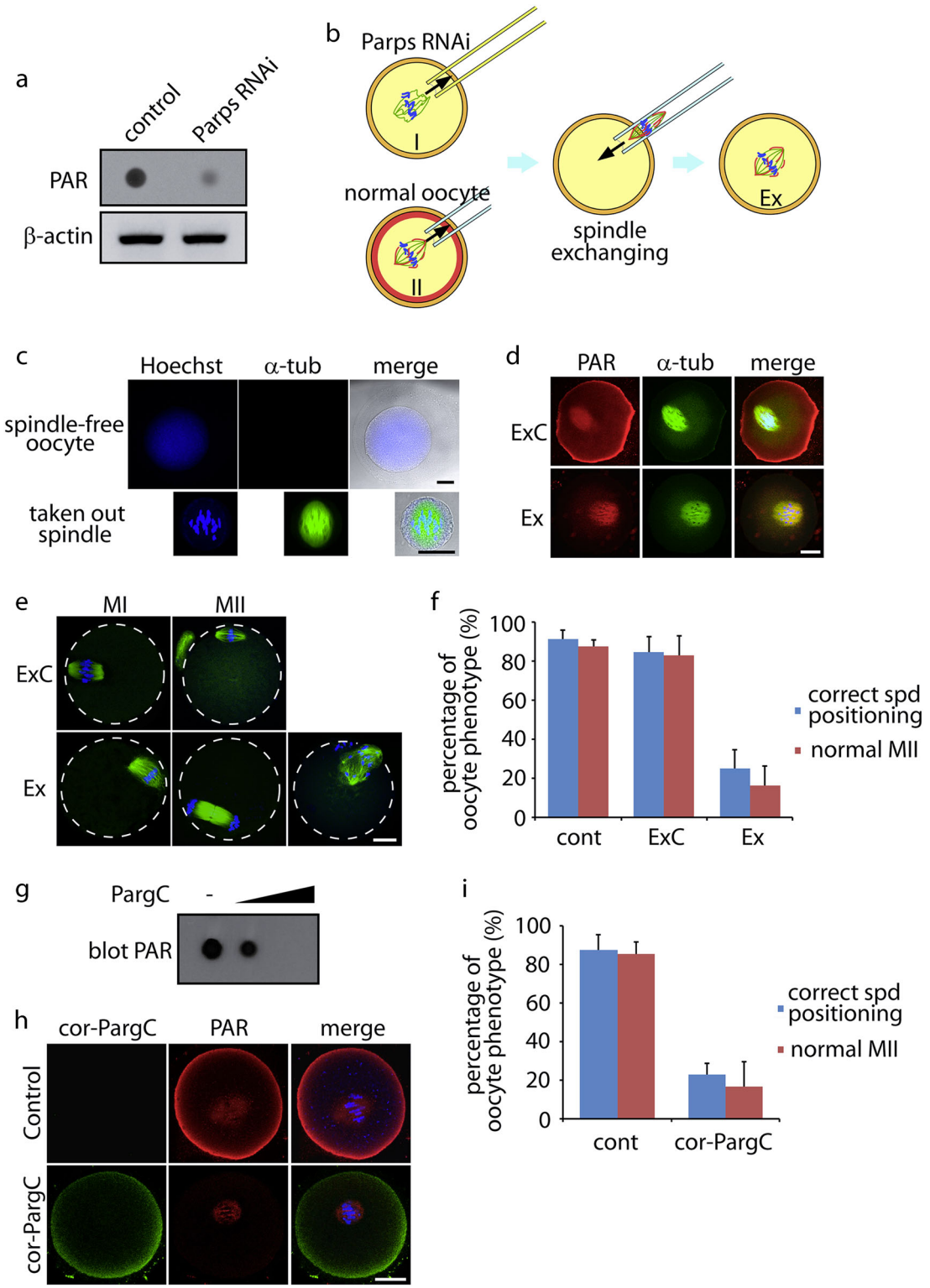

versus the cortex, we established a "spindle exchange" assay in which PAR at the spindle is maintained while the cortical PAR is specifically removed. One oocyte (oocyte I) was treated with Parp small interfering RNA (siRNA). During pro-MI, the impaired spindle in oocyte I was taken out by micromanipulation. Meanwhile, a normal spindle was taken from a non-treated oocyte (oocyte II) and placed in the spindle-free oocyte (oocyte I) to create a hybrid oocyte (oocyte Ex) (Fig. 2b). Spindle exchange between two non-treated oocytes was used as a control (oocyte ExC). Figure 2c shows the spindle that was taken out of the oocyte and the spindle-free oocyte after micromanipulation. ExC oocytes retained PAR at both cortex and spindle, whereas Ex oocytes only lacked the cortical PAR (Fig. 2d). In both ExC and Ex oocytes, spindles showed normal morphology and chromosome alignment (Supplementary information, Figure S2D and E). Additionally, the normal-functioning spindle was confirmed by testing the spindle

Fig. 2 The role of cortical PAR during oocyte asymmetric division. **a** The content of PAR in control and Parps knockdown oocytes. A total of 300 oocytes with or without the knockdown of Parps family were lysed. The lysate was split for dot blot of PAR and western blot of β-actin, respectively. In dot blot, the lysate was dropped on nitrocellulose membrane followed by the immunoblot with PAR antibody. β-Actin was used as the loading control. **b** Schematic of spindle exchange by micromanipulation. The impaired spindle in oocyte I pre-treated by Parps knockdown was removed. Meanwhile, a spindle taken out from a normal oocyte (oocyte II) was put into the spindle-free oocyte I, to generate oocyte Ex. Oocyte with spindle exchanged with another normal oocyte was used as a control (referred to as ExC oocyte). **c** The taken out spindle and the spindle-free oocyte stained with Hoechst and α-tubulin antibody. **d** Spindle-exchanged oocytes stained with PAR and α-tubulin antibodies. **e** Spindle positioning in spindle-exchanged oocytes. Ex oocytes show incorrectly positioned spindles during MI, and failure of polar body exclusion or distorted polar body during their "MII time". Dotted outline denotes the plasma membrane of the oocyte. **f** Percentage of correct spindle positioning and the rate of normal MII. "Cont" indicates normally cultured oocytes without spindle exchange. Each group of one repeat contains at least 50 oocytes. **g** Degradation efficiency of PAR by PargC. PAR was incubated with or without in vitro purified PargC. The content of PAR from the reaction solution was tested by dot blot with anti-PAR antibody. **h** Localization of cortical-PargC (GFP-Ezrin+PargC) in oocyte. Cortical-PargC was guided to the cortex, and PAR was present at the spindle but not the cortex. Normally cultured oocytes were used as a positive control. **i** Percentage of correct spindle positioning and the rate of normal MII in control and cortical-PargC-expressed oocytes. Each group of one repeat contains at least 100 oocytes. Statistical data were summarized from three independent repeats. The error bars represent the standard deviation. Scale bar, 20 μm

assembly checkpoint, which should be activated before MI and turned off after MI. In these ExC and Ex oocytes, normal mode of activation and inactivation was observed (Supplementary information, Figure S2F and G). These data indicate that neither spindle structure nor its function was impaired by the micromanipulation. Of note, most of the Ex oocytes that lost the cortical PAR showed ectopic spindles before MII. The representative phenotype was that the spindle was not able to be positioned vertical to the cortical membrane at the end of MI. Due to the incorrect spindle positioning, Ex oocytes underwent abnormal division during their "MII time", displaying the failure of polar body exclusion or a distorted polar body (Fig. 2e). The percentages of oocytes with correctly positioned spindle and the rates of normal MII in each group were summarized in Fig. 2f. These data suggest that the cortical PAR in the oocyte might mediate the spindle movement for asymmetric division during oocyte meiosis.

To further test this possibility, we expressed Parg to remove the cortical PAR. In oocytes, Parg is associated with the spindle after GVBD (Supplementary information, Figure S2H). To guide Parg specifically to the cortex for PAR degradation, a membrane-targeting peptide Ezrin[30,31] was fused with the PargC and an EGFP tag (referred to as cortical-PargC). Purified PargC could efficiently degrade PAR in vitro (Fig. 2g). We then expressed the cortical-PargC in oocytes. As shown in Fig. 2h, cortical-PargC was specifically localized at the oocyte cortex, resulting in the degradation of cortical PAR, whereas PAR on the spindle was not affected. Most of the oocytes expressing cortical-PargC showed abnormal asymmetric division with ectopic spindles before MII, and the normal MII rate was significantly lower than that in control oocytes (Fig. 2i). Taken together, these results indicate that the cortical PAR is required for the correctly eccentric localization of the spindle to ensure the asymmetric division of oocytes.

Polar array microtubules contribute to the physical contact between the spindle and the cortex

Since cortical PAR is required for the eccentric spindle positioning, we hypothesized that certain kind of microtubules emanating from the spindle could contact the cortical PAR during this process. Spindle microtubules consist of kinetochore microtubules (kMTs) and non-kMTs. Different from mitotic spindle microtubules, which contain comparable amounts of kMTs and non-kMTs, the meiotic spindle microtubules comprise around 95% non-kMTs,[32,33] which leaves numerous free plus ends in the oocyte. Of note, polar array microtubules (a kind of non-kMTs) were clearly found around the spindle in the oocyte even though the length of the fibers was short (Fig. 3a). Further, we stained for EB3, the hub for microtubule plus-end tracking proteins (+TIPs),[34] to show the fibers more clearly (Fig. 3b). Before the spindle migrated to the cortex, the polar array microtubules formed outstretched fibers around the spindle poles (Fig. 3c, top). As the spindle approached the cortex, these polar array microtubules contacted with the cortex and seemed to anchor into the cortex (Fig. 3c, bottom). By co-staining for EB3 and PAR, clear array and plus ends of the microtubules were observed to extend to the cortex (Fig. 3d, top). When the spindle approached the cortex, the microtubule plus ends penetrated into the matrix of the cortical PAR (Fig. 3d, bottom). Interestingly, EB3 displayed an unequal distribution between the two poles when the spindle was approaching the cortex, that is, heavier EB3 was loaded onto the juxtacortical pole (Fig. 3e). To exhibit more detailed information, we built three-dimensional models using the Imaris program. In the modeled oocyte labeled by Hoechst, EB3, and UtrCH-GFP (a probe that specifically binds to F-actin[35]) clear polar array microtubules led by EB3-labeled plus ends embedded in the cortex and the plasma membrane. Consistent with the staining results, the total EB3 showed an asymmetric distribution in which juxtacortical spindle pole had a heavier load (Fig. 3f). In addition, larger aggregations of EB3, which tend to represent the plus-end-localized EB3, were found localized at the juxtacortical pole of the spindle (Fig. 3g). When the spindle reached the cortex, a large number of plus-ended microtubules completely inserted into the cortex, stabilizing the spindle at the cortical area (Fig. 3h). These findings indicate that polar array microtubules contribute to the physical contact between the spindle and the cortex during oocyte meiosis.

The spindle is stabilized at the cortex during MII before fertilization. Upon fertilization, oocytes complete asymmetric division of meiosis and transit to symmetric division of mitosis. We therefore observed the cellular distribution of PAR in fertilized oocytes. Notably, the cortical PAR of the zygote showed a partial loss that occurred especially at the area above the position of the previous MII spindle (Supplementary information, Figure S3A, dashed line boxed), where PAR was intensely present before fertilization (Fig. 1g). Further, the thickness of cortical PAR (both the non-extended thickness "a" and the extended thickness "b") became thinner than that of meiotic oocytes (Supplementary information, Figure S3B). More importantly, when the fertilized egg formed the spindle for the first mitosis, PAR was not always (with a random rate) present on both of the cortical areas vertical to the spindle long axis (Supplementary information, Figure S3C), implying that cortical PAR becomes unnecessary for spindle positioning after fertilization. As centriole is still absent in the fertilized oocyte,[8,36] resulting in short polar microtubules which are similar to that in the meiotic oocyte, we were curious about how the short polar microtubules from both poles of the spindle could reach the cortex to fulfill the symmetric division. Interestingly, the fertilized oocyte assembled a spindle significantly longer than that in the meiotic oocyte (Supplementary information, Figure S3D). This finding is consistent with earlier observations

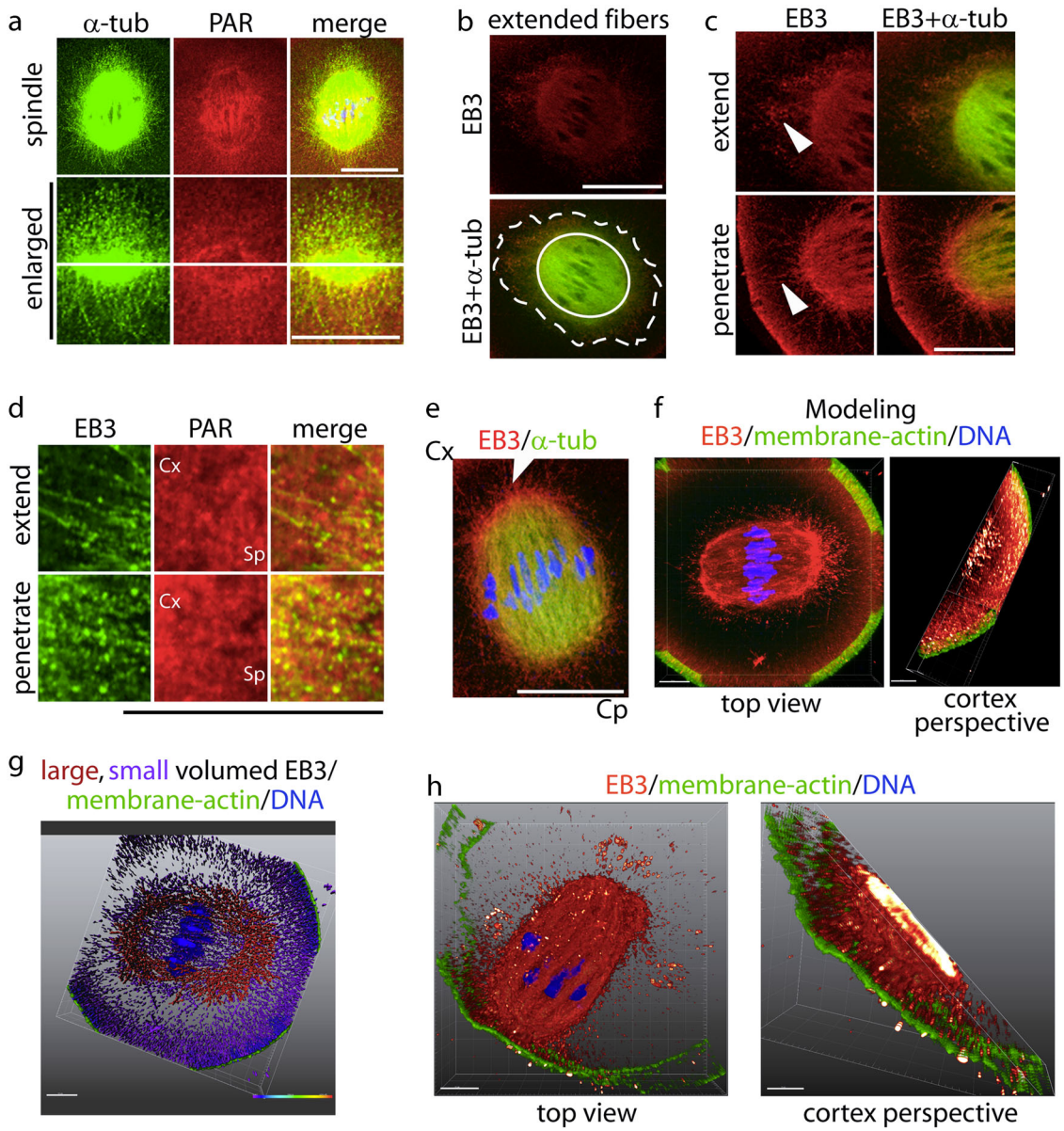

Fig. 3 Microscopy imaging of polar array microtubules and PAR during spindle migration. **a** Immunofluorescence of α-tubulin and PAR in meiotic oocytes. Polar array microtubules are found emanating from the spindle poles. **b**, **c** Immunofluorescence of EB3 and α-tubulin during spindle migration. Solid and dashed circles denote the main spindle body and the surrounding polar array microtubules with plus ends, respectively. Microtubule fibers especially the plus ends (arrowhead) marked by EB3 extend to the cortex. When spindle approaches the cortical area, polar array microtubules (arrowhead) penetrate into the cortex. **d** Close-up of EB3 and PAR immunostaining at oocyte cortex. When spindle migrates to the cortex, microtubules extend to cortical PAR and the plus ends interlace with PAR. "Cx" and "Sp" denote the side of cortex and spindle, respectively. **e** Immunostaining of EB3 and α-tubulin shows an asymmetric distribution of EB3 between the two spindle poles. The juxtacortical pole has heavier EB3 indicated by arrowhead. "Cx" and "Cp" denote the side of cortex and cytoplasm, respectively. **f** 3D display by Imaris program shows asymmetric distribution of EB3-marked microtubules and plus ends. Top view of whole-oocyte and perspective of cortical part are shown, respectively. **g** 3D display of different sized aggregators of EB3 surrounding the spindle. The larger volume of EB3 aggregators tend to be localized around the juxtacortical pole of the spindle. **h** 3D display of the spindle when it reaches at cortex. A large number of polar array microtubules headed by the plus ends (marked by EB3) penetrate into the cortex. Scale bar of immunofluorescent staining, 20 μm. Scale bar of 3D models, 10 μm

that fertilized oocytes possess longer spindles.[37] Due to the elongated spindle, polar array microtubules from both spindle poles can reach and contact with the cortex and the membrane (Supplementary information, Figure S3E). However, the interlaced colocalization between PAR and microtubule ends at the cortex was not found in fertilized eggs (Supplementary information, Figure S3E), which was much different from that in meiotic oocytes (Fig. 3c). It is intriguing but reasonable since in this way, the fertilized oocyte can remedy the flaw of centriole absence inherited from the previous meiosis and achieve the symmetric division during its first mitosis. Besides the long spindle, we found that fertilized oocytes contained multiple developed microtubule-organizing centers (MTOCs) forming over the spherical cortex as shown by microscopic scan of the Z-stack (Supplementary information, Figure S3F). The extended microtubules from the MTOCs may provide more physical links for the spindle that further stabilizes the spindle at the center of the egg during the first mitosis.

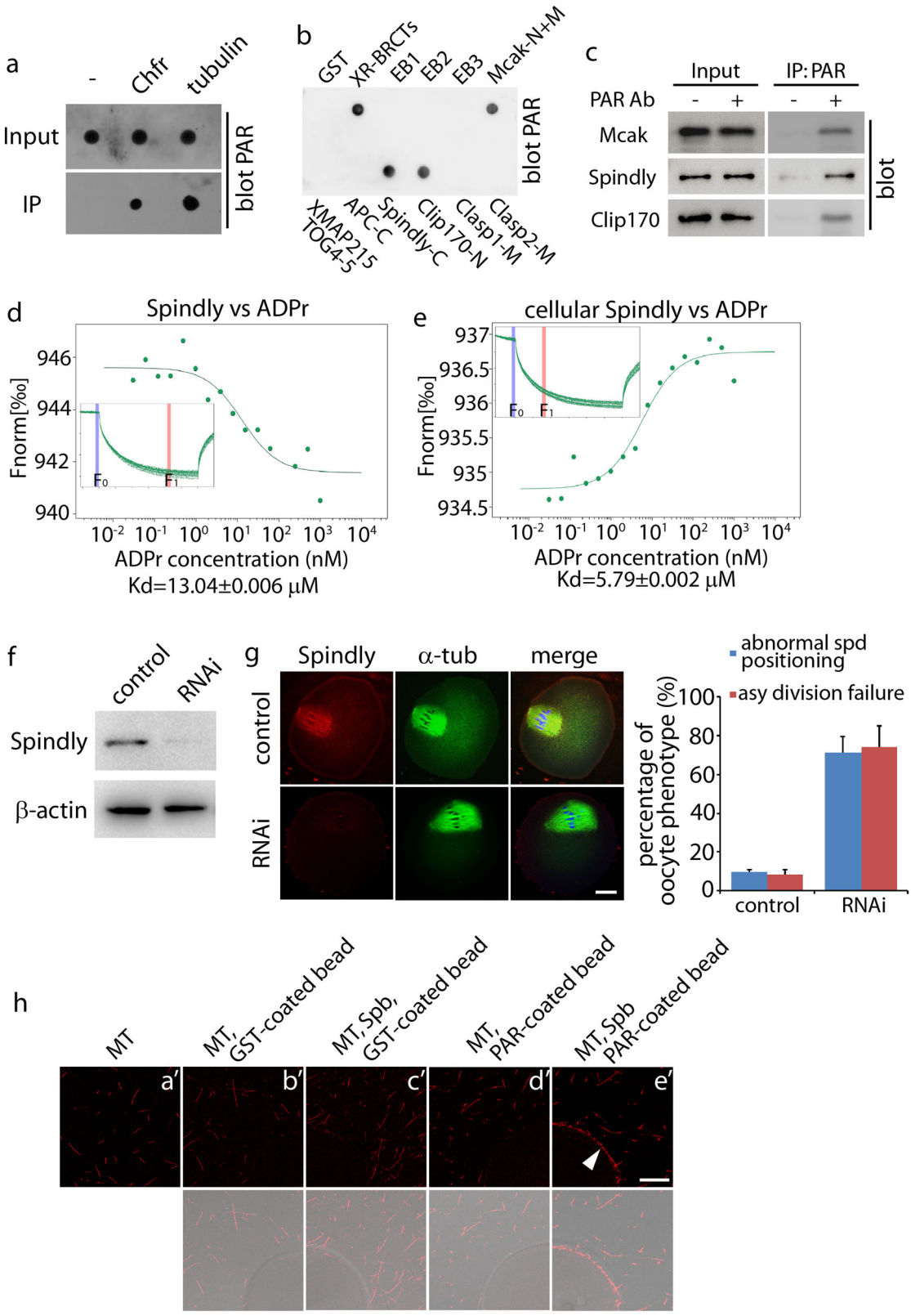

Microtubule-associated proteins link the spindle to cortical PAR

Since polar array microtubules contribute to the physical contact between the spindle and the cortex, and the cortical PAR is required for the correct positioning of the spindle, we hypothesized that microtubules may bind to the cortical PAR to facilitate the spindle migration/docking and the oocyte asymmetric division. Mouse MI oocytes were harvested and lysed followed by immunoprecipitation with α-tubulin antibody. The immunoprecipitate was blotted by PAR antibody. As shown in Fig. 4a, microtubules and PAR associated in the cell lysate. Next, we tested

Fig. 4 Microtubule-associated proteins link the spindle to PAR. **a** In vivo interaction assay between tubulin and PAR. Meiotic oocytes were lysed and then subjected to immunoprecipitation with by α-tubulin antibodies followed by dot blot with PAR antibody. Chfr which could bind PAR by its PBZ domain was used as a positive control. **b** In vitro-binding screening between the purified candidate proteins/domains and PAR. Spindly C-terminal (383–608 aa), Mcak middle (174–593 aa), and Clip170 N-terminal (1–350 aa) could pull down PAR in vitro. XRCC1-BRCTs domain (XR-BRCTs) was used as a positive control. GST was used as a negative control. **c** The cellular interaction between PAR and Clip170, Spindly, or Mcak was measured by co-immunoprecipitation with the indicated antibodies. Fifteen percent of whole-cell lysate was used as an input. **d** The in vitro-binding affinity between ADPr and Spindly C-terminal was tested by MST assay. Inset, thermophoretic movement of fluorescently labeled proteins. $F_{norm} = F_1/F_0$ (F_{norm}: normalized fluorescence; F_1: fluorescence after thermodiffusion; F_0: initial fluorescence or fluorescence after *T*-jump). K_d, dissociation constant. **e** The binding affinity of ADPr and cellular EGFP-Spindly was tested by MST. *EGFP-Spindly* plasmid was transfected into HeLa cells. The affinity between the fluorescent Spindly and ADPr was measured by MST. Inset, thermophoretic movement of fluorescent EGFP-Spindly. **f** Western blot of Spindly in the control and Spindly knockdown oocytes. β-Actin was used as a loading control. **g** The phenotypes of oocytes in the control and Spindly knockdown oocytes. The rates of abnormal spindle positioning and failure of asymmetric division were summarized in the histogram. Each group of one repeat contains at least 50 oocytes. The error bars represent the standard deviation. **h** Microtubules are captured by PAR in the presence of Spindly PAR-binding region. Rhodamine-labeled tubulins were polymerized to fluorescently dynamic microtubules in vitro (**a'**), and incubated with GST-coated beads (**b'**, **c'**), or PAR-coated beads (**d'**, **e'**), with or without the addition of the purified Spb (Spindly PAR-binding region). Only PAR-coated beads were able to capture and trap the microtubules, and this process required Spb. Arrowhead indicates the PAR-captured microtubules on the bead surface. Bright-field images of the beads are shown at the bottom. Scale bar, 20 μm

whether microtubules and PAR bind with each other directly. Purified tubulins and PAR were incubated with α, β-tubulin antibodies and protein G sepharose in tubulin polymerization reaction buffer. However, tubulins could not immunoprecipitate PAR in vitro (Supplementary information, Figure S4A). To confirm this result, the direct interaction between tubulin and PAR was further examined by microscale thermophoresis (MST).[38,39] Due to the inconsistent length among individual PARs and polytropic formations of branches in the polymer, PAR is endowed high level of heterogeneity that is not suitable for the MST assay.[19,40] Thus, the structural and functional unit of PAR, ADP-ribose, was used. Again, no binding signal between the purified tubulin and ADP-ribose was detected and the dissociation constant (K_d) was over 500 μM (Supplementary information, Figure S4B). We thus hypothesized that certain microtubule-associated protein(s) might bind PAR directly, which linked PAR to microtubules. Since only non-kMTs could extend to the cortex, it was very likely that the microtubule-associated protein(s) localized at the microtubule plus ends. On the other hand, each ADP-ribose contains two negatively charged phosphate groups, and thus PAR, the polymer of ADP-ribose, contains substantial amounts of negative charges. Based on these notions, 10 potential candidates were selected (Supplementary information, Figure S4C) including both the core microtubule-associated proteins which mainly act on the plus-end[41,42] and the microtubule-binding proteins with obvious positive charges.[43–45] Recombinant proteins or domains were expressed in vitro and the interaction with PAR was screened by dot blot. Three candidates (Spindly, Mcak, and Clip170) bound to PAR (Fig. 4b). To validate the in vitro data, the cellular interaction between PAR and these proteins was tested by co-immunoprecipitation. As expected, PAR could co-immunoprecipitate Spindly, Mcak, and Clip170 in meiotic oocytes, respectively (Fig. 4c). To further confirm the direct interaction between the proteins and PAR, the binding affinity and K_d were examined by MST in vitro. Notably, Spindly showed an obvious binding curve to ADP-ribose with a K_d of 13.04 μM (Fig. 4d). Mcak and Clip170 also interacted with ADP-ribose with a K_d of 46.37 and 52.59 μM, respectively (Supplementary information, Figure S4D and E). As Spindly showed a high affinity to PAR in vitro, we were curious whether it is the same in cell. GFP-Spindly was expressed in HeLa cells followed by lysing. The affinity between the fluorescent Spindly in the lysate and the ADP-ribose was measured by MST. Notably, cellular GFP-Spindly interacted with ADP-ribose, and the K_d was 5.79 μM (Fig. 4e).

To validate the biological effect of PAR on microtubules, we established an assay (here named "microtubule capture assay") in which the direct interaction between PAR and dynamic microtubules could be examined. Microtubules were polymerized from tubulins and rhodamine-labeled tubulins in vitro. These dynamic microtubules were incubated with control (glutathione *S*-transferase (GST)-coated) or PAR-coated beads. Few microtubules could be attracted by control beads regardless of the addition of the purified PAR-binding region of Spindly (Spb), Mcak (Mpb), and Clip170 (Clpb) (Fig. 4h; Supplementary information, Figure S4F). However, the microtubules were tightly attracted and captured by the PAR-coated beads in the presence of Spb (Fig. 4h). This phenomenon was also observed when Spb was replaced by Mpb or Clpb, though the capture ability mediated by Mpb or Clpb was weaker than that by Spb (Supplementary information, Figure S4F and G). These results suggest that cortical PAR mediates spindle migration and oocyte asymmetric division by interacting with microtubule-associated proteins including Spindly, Mcak, and Clip170, and among them Spindly has the highest affinity with PAR. To validate the cellular function of Spindly, oocyte Spindly was knocked down. Western blot results proved the efficient knock down (Fig. 4f). As expected, most of the oocytes in Spindly RNAi group showed an ectopic spindle at MI stage (71.4%) and a failure of asymmetric division (74.0%) (Fig. 4g). These data suggest that microtubule-associated proteins link the spindle to the cortical PAR.

A PAR-binding domain restores the asymmetric division of Spindly knockdown oocytes

To confirm the cellular function of the physical link between the spindle and the cortical PAR, we fused the PAR-binding domain of Spindly (Spb, 383–608 amino acids) to EB3, which per se does not bind PAR. The successful expressions of EGFP-EB3 and EGFP-EB3 +Spb in oocytes were confirmed by western blot against EB3 (Fig. 5a). To test the binding ability of these proteins, they were expressed with His-tag and purified in vitro. As expected, the purified EB3 could then interact with PAR directly when fused with Spb (Fig. 5b). The binding ability was also validated by the MST assay, with the K_d (EB3+Spb versus ADPr) of 15.14 μM (Fig. 5c, d). Next, to test whether EB3+Spb could rescue the failure of asymmetric division in Spindly knockdown oocytes in which the interaction between the spindle and the cortex was impaired (Fig. 4g), we expressed EGFP-EB3 or EGFP-EB3+Spb in these Spindly depleted oocytes. The expression of EGFP-EB3 did not rescue the abnormal spindle positioning and the failure of asymmetric division (Fig. 5f, g, j). Intriguingly, when EB3+Spb was expressed in these oocytes, the spindle was positioned correctly at the cortex, followed by a successfully asymmetric division (Fig. 5h, j). On parallel, a previously identified PAR-binding domain, PAR-binding zinc-finger (PBZ) of APLF (368–444 amino acids)[26] was fused to EB3 (Fig. 5a, b, e). Similar to EB3+Spb, EB3 +PBZ was able to restore the spindle positioning and the

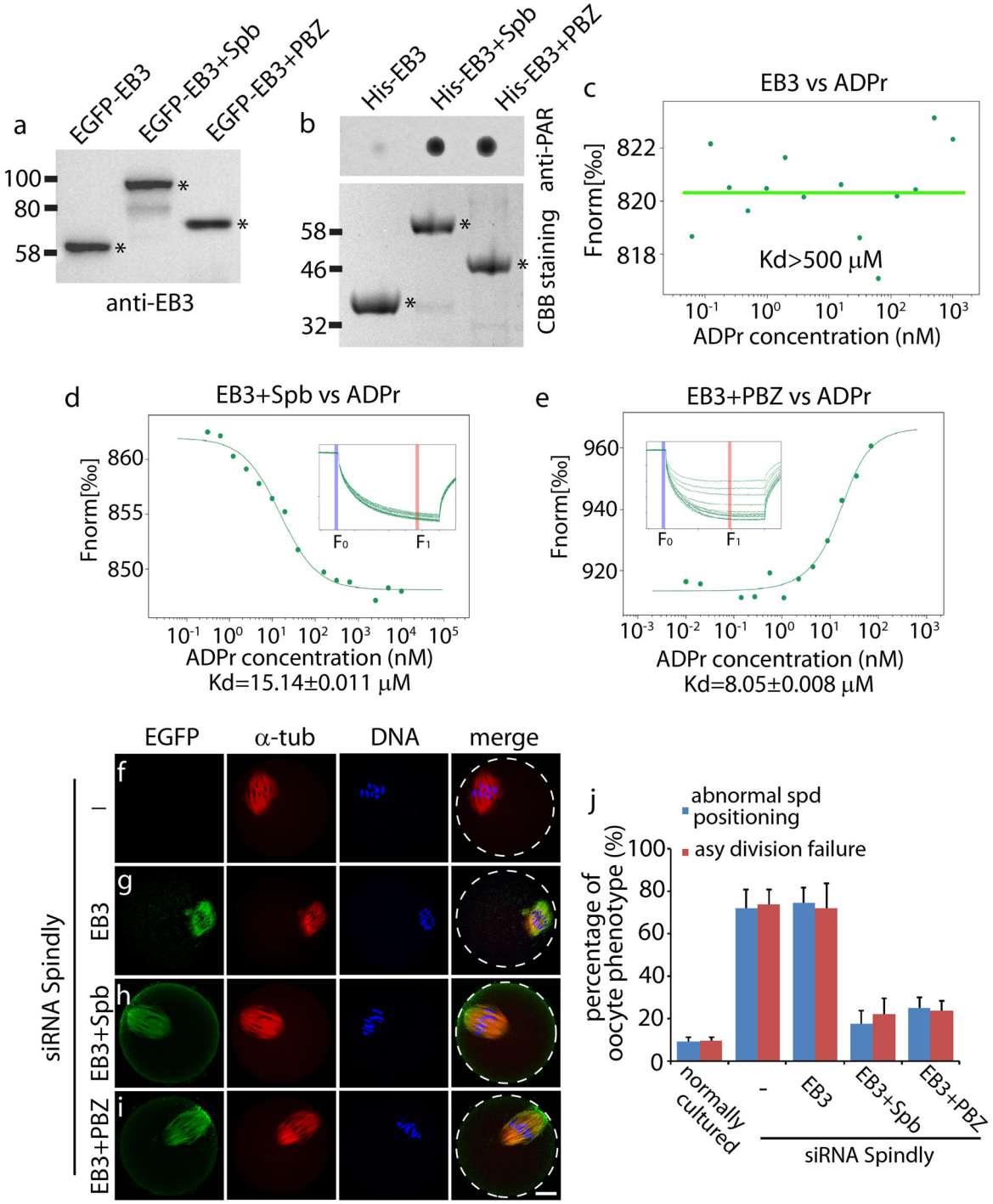

Fig. 5 A PAR-binding domain re-links the spindle to the cortex in Spindly deficient oocytes. **a** Expression of EGFP-EB3, EGFP-EB3+Spb, and EGFP-EB3+PBZ in mouse oocytes. Oocytes expressing the fused proteins were lysed followed by western blot with EB3 antibody. EGFP-EB3 (60.6 K_d), EGFP-EB3+Spd (86.2 K_d), and EGFP-EB3+PBZ (69.4 K_d) were successfully expressed in oocytes. Asterisks denote the indicated blot bands. **b** In vitro-binding assay between PAR and EB3, EB3+Spd, and EB3+PBZ. The purified EB3, EB3+Spd, or EB3+PBZ with His-tag was incubated with PAR. EB3+Spd and EB3+PBZ but not EB3 could pull down PAR. CBB staining, Coomassie brilliant blue staining. **c**–**e** The in vitro-binding affinity between ADPr and His-EB3, EB3+Spd, or EB3+PBZ was tested by the MST assay. Inset, thermophoretic movement of fluorescently labeled proteins. $F_{norm} = F_1/F_0$ (F_{norm}: normalized fluorescence; F_1: fluorescence after thermodiffusion; F_0: initial fluorescence or fluorescence after *T*-jump). K_d, dissociation constant. **f**–**i** Function of the PAR-binding domain in Spindly deficient oocytes. EGFP-EB3, EGFP-EB3 +Spb, or EGFP-EB3+PBZ was expressed in Spindly knockdown oocytes, respectively. The expression of EB3+Spb or EB3+PBZ could re-position the spindle correctly and achieve the asymmetric division. Scale bar, 20 μm. **j** Rates of the abnormal spindle positioning and the failure of asymmetric division in each group were summarized. Error bars represent the standard deviation

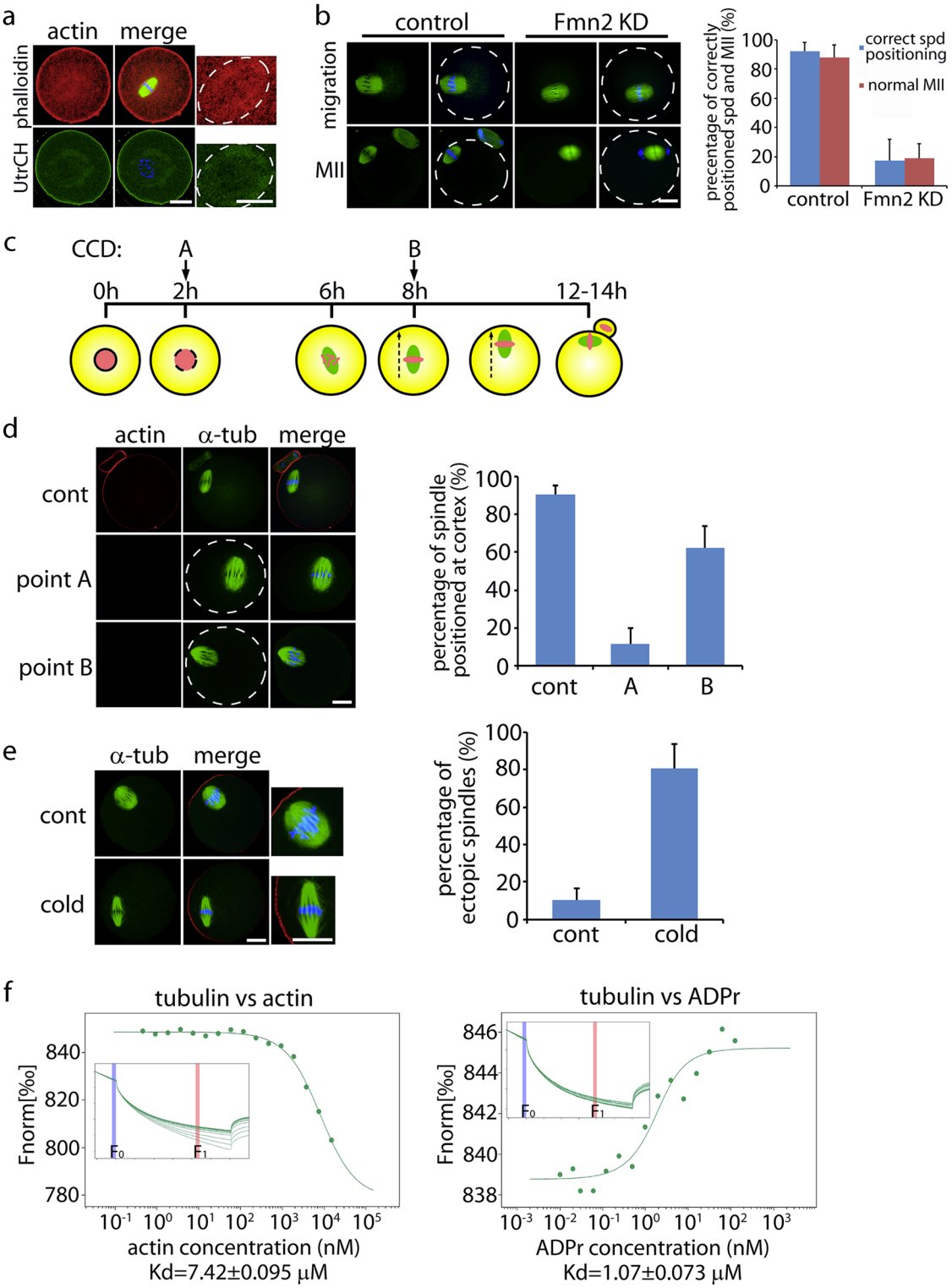

Fig. 6 Actin and PAR sequentially regulate spindle positioning. **a** Actin staining by phalloidin and UtrCH in meiotic oocytes. For UtrCH fluorescence, in vitro transcribed-cRNA of GFP-UtrCH from the linearized DNA was microinjected into oocytes followed by fluorescent microscopy. The enlarged images show cytoplasmic F-actin surrounding the spindle. **b** Spindle positioning in control and Formin2 knockdown oocytes. Percentages of correctly positioned spindles and MII rates were counted. **c** Schematic of timepoints of CCD treatment during oocyte meiosis. **d** Spindle positioning in the control and CCD-treated groups. Percentages of spindles positioned at the cortex were counted. Circle of dashed line denotes the oocyte outline. **e** Staining of microtubules and actin in control and cold-treated oocytes. Percentages of ectopic spindles were counted. Each group of one repeat contains at least 50 oocytes for **b**, **d**, and **e**. Scale bar, 20 μm. **f** MST-binding assay of cellular tubulins to actin or ADPr. Inset, thermophoretic movement of fluorescent α-tubulin. $F_{norm} = F_1/F_0$ (F_{norm}: normalized fluorescence; F_1: fluorescence after thermodiffusion; F_0: initial fluorescence or fluorescence after *T*-jump). K_d, dissociation constant

asymmetric division in the Spindly depleted oocytes (Fig. 5i, j). These results further confirm the critical role of microtubule-associated proteins containing a PAR-binding domain, such as Spindly, in oocyte asymmetric division.

The different roles of PAR and actin during spindle positioning

Since the centriole is absent and, as a result, the polar array microtubules are not fully developed in the oocyte, the role of microtubules per se for spindle positioning during asymmetric division has always been ignored. Previous studies emphasized the roles of actin in this process. However, these models are inconsistent and two distinct kinds of F-actin forces (pushing and pulling) have been proposed.[3,5,15–17] To define the role of actin in asymmetric division, we stained the mouse oocyte with phalloidin (for general actin) or UtrCH-GFP, a probe that specifically binds to F-actin.[35] After GVBD, both phalloidin and UtrCH-GFP in the cytoplasm were found around the spindle but not in the subcortex (Fig. 6a), implying a pushing but not a pulling force around the spindle. Since Formin2 was reported to nucleate actin filaments surrounding spindle,[16,17] we knocked down Formin2 in oocytes (Supplementary information, Figure S5A) and examined spindle behavior. As expected, loss of Formin2 resulted in the failure of spindle migration, and most of the spindles stayed at the pericenter of oocytes. About 10–12 h after GVBD, more than 80% of Formin2 knockdown oocytes could not exclude the polar bodies. Instead, a subset of them (34.8%) "excluded" the polar bodies into the oocytes (Fig. 6b). These data suggest that the pushing force generated by actin is a critical trigger for symmetry breaking of spindle migration, which is consistent with the previous reports.[16,17]

As the contact between polar array microtubules and cortical PAR is required for spindle eccentric positioning, we hypothesize that actin and PAR sequentially regulate oocyte asymmetric division in which actin breaks the centric position of spindle at the beginning, and the interaction between polar array microtubules and cortical PAR facilitates the later migration and stabilizes the spindle at the cortex. Previous studies have shown that cytochalasin D (CCD) could impair F-actin and thus spindle migration.[16] To elaborate the role of F-actin in this process, a non-inhibited window was left for F-actin to function normally during the initial phase of spindle migration. We began the CCD treatment at the early period of MI when the chromosomes had completed their alignment but visible spindle migration had not yet occurred (Fig. 6c, timepoint B). This treatment point was delayed by hours compared with that in previous studies (Fig. 6c, timepoint A). Interestingly, although few oocytes reached MII, 62% of the spindles in point B-treated group were able to migrate to the cortex, while most of spindles in point A-treated group could not move to the cortex (Fig. 6d), suggesting that F-actin mainly functioned in the early period during the spindle migration. To rule out the possibility that CCD treatment might affect PAR, the distribution of PAR in meiotic oocytes receiving CCD treatment was examined by immunofluorescence. CCD did not show an effect on PAR in the oocytes (Supplementary information, Figure S5B). Reciprocally, we also performed a cold treatment experiment[46] to examine the role of polar array microtubules in the late period during the spindle migration. non-kMTs are more sensitive to cold treatment compared with kMTs, that is, non-kMTs (polar array microtubules in oocyte) disassemble while kMTs cluster together and persist as cold-stable bundles.[46] Conversely, the polymerization of actins is not as sensitive to temperature as that of tubulins, and actin polymerization can occur across a broad range of temperatures.[47,48] Here, oocytes were cultured to MI, and then subjected to cold treatment followed by immediate fixation. Of note, 80.5% oocytes upon cold treatment exhibited ectopic spindles, a ratio much higher than that in non-cold-treated group (Fig. 6e). Among the ectopic spindles, 51.7% could still move to or near the cortical area, but with wrong orientation, which probably resulted from the migration inertia by the F-actin-pushing stream. These data suggest that polar array microtubules are important for the spindle migration and stabilization at the cortex.

Since PAR and actin are both required for spindle positioning, we compared the affinity of microtubules and PAR, with the affinity of microtubules and actin. MST results showed that both ADP-ribose and actin had obvious association with cellular microtubules. Notably, the affinity of ADP-ribose to microtubules was seven times higher than that of actin to microtubules (Fig. 6f), indicating that the force between PAR and microtubules is much stronger than that of actin and microtubules. It is not surprising since before the drastic process of asymmetric division, oocyte requires a substantial physical interaction between the cortex and the spindle that ensures the dock and stabilization of the spindle to the cortex. These results suggest that actin and PAR sequentially regulate spindle positioning. Cytoplasmic actin mainly functions for breaking the symmetric position of the spindle by launching an initial pushing force, while cortical PAR acts as a physical link for spindle microtubules to dock and stabilizes the spindle at the cortex.

DISCUSSION

PAR has been studied for over decades and believed to mainly function under cellular stress conditions such as DNA damage.[20–22] Until now, 17 PARP members have been identified in human, and PARP1 is the best studied among these polymerases.[22,40] Upon genomic stress, the enzymatic activity of PARP1 increases around 500-fold to synthesize PAR.[19] However, other members of PARPs may function beyond the genomic stress since they do not possess the DNA-binding domain as PARP1.[22,49] Interestingly in this study, we show an intensive staining of PAR at mouse oocyte cortex, implying a unique role of this molecule in female germ cells. To retain most maternal materials for the fertilization and early embryonic development, oocytes undergo a highly asymmetric division during the meiosis. The asymmetric division in oocytes is much different from those in other types of cells because of the large volume of oocytes and their non-adherent growing property. Thus, oocytes must own their unique molecule(s), especially at the cortex, for the special division. As each ADP-ribose residue contains two phosphate groups carrying two negative charges,[40] the oocyte cortical layer of PAR therefore contains an enormous amount of negatively charged groups and provides enough avidity to dock positively charged microtubule-associated proteins therefore capturing the spindle. The high affinity between PAR and the microtubule-associated protein Spindly supports this conclusion. Of note, the cortical PAR in oocytes may fit into an emerging concept of "phase separation," one of the most exciting concepts developed recently in cell biology. This concept emphasizes the polymeric structures, electric fields, and large-scale molecule interactions in cellular context.[50–52] The branched polymeric structure and the huge negative charges endow PAR physical features needed to be qualified as a unique phase to perform its biological functions in oocytes. Another interesting observation is that not all mouse oocytes at the GV stage show a positive nuclear staining for PAR as demonstrated in Fig. 1b. Instead, some oocytes exhibit a nuclear envelope staining (Supplementary information, Figure S1C). This difference should be related to some regulation of genome or transcription but not asymmetric division, which warrants future investigation.

Till now, it is still unclear why mammalian oocytes lack centrioles and long polar array microtubules. In mitotic cells, the long-developed astral microtubules emanating from the centrioles of both spindle poles can contact the cortex synchronously, enabling cells to adjust and keep the spindle at the center[14,53] (Fig. 7a). Interestingly, the polar array microtubules in oocytes are less developed and thus much shorter. Given the huge volume of

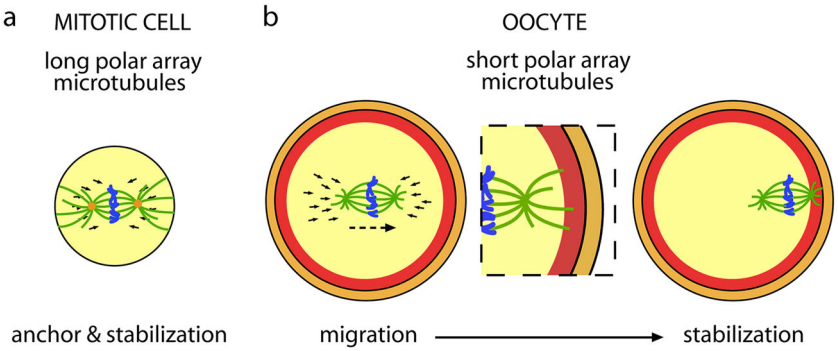

Fig. 7 A model for asymmetric division of mammalian oocytes. **a** Due to the well-developed astral microtubules emanating from two spindle poles in mitotic cells, the spindle can be adjusted and positioned at the cell center by the direct interaction between the astral microtubules and the cortex. **b** In mammalian oocytes, because of the absence of centriole, the polar array microtubules are not developed long to reach the cortex. The "floating" spindle is always passively struck by the cytoplasmic push of actin. Once the spindle deviates from the center, the polar array microtubules emanating from the juxtacortical pole of the spindle interact with cortical PAR, which docks and stabilizes the spindle to the cortex. Orange dots in mitotic cell, centrioles; green, microtubules; red, PAR; black arrows, actin-pushing force

oocytes compared to that of somatic cells, it makes oocyte cortex more "synchronously unreachable" for the polar array microtubules from both of the spindle poles. Previous reports highlight the contributions of actin during spindle positioning to the cortex and the asymmetric division.[4,5,15–17] However, a unified theory has not been established since these studies lead to conflicting models, such as a pulling force for the spindle positioning mediated by cortical actin between the membrane and the spindle,[5] or a pushing force surrounding the spindle generated by F-actin in the cytoplasm.[15,18] In our study, we re-investigated the distribution of actin by fluorescent microscopy using both phalloidin staing and UtrCH-GFP. It is worth noting that a positive signal surrounding the spindle rather than at the cortical area was found. The knockdown of Formin2, which nucleates actin filaments surrounding the spindle,[16,17] resulted in the failure of oocyte asymmetric division. Moreover, treating oocytes with CCD during the late spindle migration when one spindle pole already approaches the cortex did not affect the spindle cortically positioning. These findings further confirm the contribution of the actin-pushing force.

In our model (Fig. 7b), the spindle deviates away from the center region of the oocyte by the dynamic push of the cytoplasmic actin. When approaching the cortex, the short polar array microtubules from the juxtacortical spindle pole catch cortical PAR, which eventually docks and stabilizes the spindle at the cortex. Three microtubule-associated proteins, that is, Spindly, Clip170, and Mcak, have been identified to bind PAR. As expected, all the three proteins have positively charged regions or domains.[45,54,55] These and other microtubule-associated proteins with positive charges help explain the high affinity between PAR and cellular microtubules. The physical link between the spindle and cortical PAR ensures the firmly cortical positioning of the spindle during the drastic cytokinesis of the asymmetric division. Thus, our work demonstrates a comprehensive model for oocyte asymmetric division and provides potential targets for clinical oocyte maturation failure and women infertility.

MATERIALS AND METHODS

Chemicals and antibodies

All chemicals were purchased from Sigma except for those specifically mentioned. Purified PAR used for in vitro assay was purchased from Trevigen. Anti-PAR antibodies were purchased from Millipore (MABC547, for results in the full paper) and Trevigen (4335-MC-100, for the result in Supplementary information, Figure S1A). Anti-Parp1 (ab6079), anti-Parg (ab16060), anti-EB3 (ab157217), anti-Formin2 (ab72052), and anti-Clip170 (ab106524) antibodies were purchased from Abcam. Anti-Spindly (MABT106) and anti-Mcak (NBP2-01064) antibodies were purchased from Millipore and Novus, respectively. Rhodamine phalloidin (R415) was purchased from Thermo Fisher Scientific.

Plasmid and constructs

For fusion protein or domain expression, mouse EB1, EB2, and EB3 were cloned into pET-21a or pET-28a. Mouse Spindly C terminus (383–608 aa), Mcak neck+motor (174–593 aa), Clip170 N terminus (1–350 aa), Clasp1 SXIP-containing region (496–790 aa), Clasp2 SXIP-containing region (497–794 aa), adenomatous polyposis coli C terminus (2,223–2,843 aa), Ckap5/XMAP215 TOG4-5 (1,079–1,428 aa), and Parg catalytic domain (444–961 aa) were cloned into pGEX-4T-1 or pGEX-6P-1. EB3+Spb and EB3+PBZ were cloned into pET-28a. For protein expression in mouse oocytes, the indicated gene or fusion gene was cloned into pcDNA3-EGFP.

Oocyte collection and culture

Mice care and handling were conducted in accordance with policies promulgated by the Ethics Committee of Peking University Third Hospital. Female ICR mice (4–6 weeks) were sacrificed by cervical dislocation after intraperitoneal injections of five intrauterine pregnant mare serum gonadotropin for 44–46 h. Immature oocytes arrested at prophase of meiosis I were collected from ovaries in the M2 medium. Only those immature oocytes displaying a clear GV were selected and cultured in the M16 medium under liquid paraffin oil at 37 °C in an atmosphere of 5% CO_2 in air. Oocytes were collected for subsequent experiments at the appropriate stages or timepoints during the culture.

Dot blot of PAR in mouse oocytes

Mouse oocytes were cultured to GV, GVBD, pro-MI, MI, and MII, respectively. After lysis with RIPA buffer, the lysate was spotted onto a nitrocellulose membrane. After drying in air, the membrane was blocked with (Tris-buffered saline with Tween) TBST buffer (0.15 M NaCl, 0.01 M Tris-HCl, pH 7.4, 0.1% Tween-20), supplemented with 5% milk, and extensively washed with TBST. Then, the membrane was incubated with anti-PAR antibody (1:1,000) overnight at 4 °C. After washing three times in TBST, the membrane was incubated with the horseradish peroxidase (HRP)-conjugated secondary antibody for 1 h at room temperature. The dot blot was detected by enhanced chemiluminescence detection system.

Recombinant protein expression and pull-down/dot-blot assay

GST or His fusion proteins or domains were expressed in *Escherichia coli* and purified under standard procedures. Pull-

down/dot-blot assay was performed according to our previous procedure.[23] In brief, purified GST or His fusion proteins (10 pmol) were incubated with PAR (100 pmol, calculated at ADP-ribose) and glutathione or Ni sepharose in 500 μL phosphate-buffered saline (PBS) buffer for 2 h at 4 °C. After washing four times, the pellets were eluted with glutathione or imidazole elution buffer for 40 min. After centrifuging, the supernatant was spotted onto a nitrocellulose membrane. After drying in the air, the membrane was blocked with TBST buffer supplemented with 5% milk and extensively washed with TBST. Then, the membrane was incubated with anti-PAR antibody (1:1,000) overnight at 4 °C. After three times of washes in TBST, the membrane was incubated with the HRP-conjugated secondary antibody for 1 h at room temperature. The dot blot was detected by enhanced chemiluminescence detection system.

PAR degradation assay

The catalytic domain of mouse Parg was expressed and purified. The recombinant protein (2 and 10 pmol for an increased dose) was incubated with PAR (100 pmol, calculated as the ADP-ribose unit) for 2 h at room temperature in 50 μL PBS buffer. After incubation, the reaction solution was spotted onto a nitrocellulose membrane. After drying in the air, the membrane was blocked with TBST buffer supplemented with 5% milk and extensively washed with TBST. Then, the membrane was subjected to anti-PAR dot-blot assay described above.

CCD and cold treatment of oocytes

For CCD treatment, oocytes at the appropriate stages were incubated in the M16 medium containing 1 μg/mL CCD. After treatment, oocytes were immediately fixed for immunofluorescent staining. For cold treatment, oocytes at the appropriate stages were cultured in the low temperature incubator at 10 °C for one and a half hours followed by immediate fix and immunofluorescent staining.

Knockdown and cRNA expression

For RNAi experiment, fully grown GV-intact oocytes were microinjected with 7–10 pL of non-targeting (control) or targeting siRNA in the M2 medium in the presence of 2.5 μM milrinone. To facilitate the depletion of mRNA by siRNA, microinjected oocytes were arrested at GV stage in the M16 culture medium in the presence of 2.5 μM milrinone around 16 h, followed by thorough washes and cultured in fresh M16 culture medium at the indicated stages or timepoints. The working concentration of Parps siRNA pool was 50 μM. The siRNA sequences of the Parps RNAi mixture are: Parp1: 5′-CCGCTGGTACCATCCAACTTGCTTT-3′, 5′-CAGAATGAGCTGATCTGGAATATCA-3′; Parp2: 5′-CCAAGCTGGGAAAGGCTCATGTGTA-3′, 5′-GGGAAAGGCTCATGTGTATTGTGAA-3′; Parp3: 5′-TAGACCCTGCCACCCAGAACCTTAT-3′, 5′-CAGAACCTTATCACCAACATCTTCA-3′; Parp4: 5′-GAGCACTGGAAAGCAAACTTCTGAA-3′, 5′-GCAAACTTCTGAAGGTGCAATTGAA-3′; Parp5a: 5′-CAACCTTGGTCAATTGCCATGGCAA-3′, 5′-ACGAAATCTGCAAACTCCTTCTAAA-3′; Parp5b: 5′-CAGATTACCTTAGATGTCCTAGTTG-3′, 5′-CATGCATACATAGGTGGCATGTTTG-3′; Parp6: 5′-AGCTCCGAGTTGGACGCCTTATGAA-3′, 5′-CAGAGCAGAGGATTCCAACGTTAAA-3′; Parp7: 5′-CACTGAACCTGAGCCAGACTGTGTA-3′, 5′-CCTGAGATCCTTGAGGCCAATATTA-3′; Parp8: 5′-CAACACGTATGTGTCAAGTTCAGAA-3′, 5′-CAAGCACCCTCAGCTAGAAGCTGAT-3′; Parp9: 5′-CAGTTACGAACAGCCAGACAGCTAT-3′, 5′-CCCTCTGGATTTGTGTACAAGCATA-3′; Parp10: 5′-CCAGAAATACCAGATGAGCTCATTA-3′, 5′-GAGCTCATTACTCTGTACTTTGAAA-3′; Parp11: 5′-CGGAATGTGGGAAGTGGCACATGTT-3′, 5′-CGAGTATAATGAAGTGGCCAGTCTT-3′; Parp12: 5′-CCGGGAAGAACTGTAGGAATGGTCA-3′, 5′-GAGTGCAAGTTTGGCACAAGCTGTA-3′; Parp13: 5′-GATCCCGAGGTATTCTGTTTCATCA-3′, 5′-AAGCGCAACTCTACGAGCTGCTGAA-3′; Parp14: 5′-ACTTGATCAACAAGTTGCAAGTGTA-3′, 5′-GCAGTGCTCTCTGGCATCAAGTCTA-3′; and Parp16: 5′-CCCGGATTTCCTATTTGAAATTGAG-3′, 5′-GAGACCAAAGGAGAACGAGACCTAA-3′ (GE, USA). The two siRNA sequences of Formin2 were 5′- CAGCTGATGGCTTTCAGAACGTGTT -3′ and 5′- CAGTCCCAAGGACGTTGATACAGAA -3′ (Invitrogen, USA). For cRNA expression in oocytes, the plasmid of F-actin probe pCS2+-UtrCH-EGFP was purchased from http://www.euroscarf.de. Ezrin+PargC (444–961 aa of Parg), EB3, EB3+Spb (383–608 aa of Spindly), and EB3+PBZ (368–444 of APLF) were subcloned into pcDNA3-EGFP. Capped cRNAs were synthesized from linearized plasmid using Sp6 or T7 mMessage mMachine kit (ThermoFisher, USA), and purified with MEGAclear kit (ThermoFisher, USA). Typically, 7–10 pL of 0.6–1.0 μg/μL cRNA was injected into oocytes for protein expression.

Immunoprecipitation and western blot

Immunoprecipitation was performed with the indicated antibodies according to the protocol of ProFound Mammalian Co-Immunoprecipitation kit (Pierce, USA). For western blot, oocytes were lysed in 4× LDS sample buffer (ThermoFisher, USA) containing protease inhibitor and boiled in water for 5 min. The proteins were separated by sodium dodecyl sulfate-polyacrylamide gel electrophoresis and then electrically transferred to polyvinylidene fluoride membranes. Following transfer, the membranes were blocked in TBST containing 5% skimmed milk for 2 h, followed by the incubation overnight at 4 °C with the indicated primary antibodies. After washing in TBST, the membranes were incubated for 1 h at 37 °C with 1:1,000 dilution of HRP-conjugated secondary antibody. Finally, protein bands were visualized by enhanced chemiluminescence detection system.

Immunofluorescent staining and confocal microscopy

Oocytes were fixed in 4% paraformaldehyde in PBS (pH 7.4) for 30 min followed by permeabilization in 0.5% Triton X-100 for 25 min at room temperature. Then, oocytes were blocked with 1% bovine serum albumin-supplemented PBS for 1 h and incubated with the indicated primary antibodies (1:200–1:500) at 4 °C overnight. After washing three times in PBS containing 0.1% Tween-20 and 0.01% Triton X-100, oocytes were incubated with an appropriate fluorescent secondary antibody for 1 h at room temperature. For the antibodies of direct-fluorescence α-tubulin and phalloidin, the incubated time was 60 min with the dilution of 1:200 and 1:600, respectively. After washing three times, oocytes were stained with Hoechst 33342 (10 μg/mL) for 15 min. Finally, oocytes were mounted on glass slides and observed under a confocal laser scanning microscope at ×63/1.40 (Carl Zeiss 710).

Microscale thermophoresis

MST was performed according to the previous work as described.[39] In brief, purified recombinant protein was labeled with a RED-NHS protein labeling kit (NanoTemper, Germany) according to standard protocol. The protein was then incubated at a constant concentration (10–50 nM) with twofold serial dilutions of actin or ADP-ribose in MST-optimized buffer (50 mM Tris-HCl, pH 7.4, 150 mM NaCl, 10 mM $MgCl_2$, 0.05% Tween-20). Equal volumes of binding reactions were mixed by pipetting and incubated for 15 min at room temperature. Mixtures were enclosed in standard-treated or premium-coated glass capillaries and loaded into the instrument (Monolith NT.115, NanoTemper, Germany). Measurement protocol times were as follows: fluorescence before 5 s, MST on 30 s, fluorescence after 5 s, and delay 25 s. For all the measurements, 200–1,000 counts were obtained for the fluorescence intensity. The measurement was performed at 20% and 40% MST power. $F_{norm} = F_1/F_0$ (F_{norm}: normalized fluorescence; F_1: fluorescence after thermodiffusion; F_0: initial fluorescence or fluorescence after T-jump). K_d values were determined with the NanoTemper analysis tool.

Microtubules capture assay

Rhodamine-labeled tubulins (10 μM, Cytoskeleton) were polymerized in vitro in G-PEM buffer (Cytoskeleton) containing 20 μM paclitaxel according to the standard procedure provided by the manufacturer. The polymerized microtubules were then incubated with beads from Protein G Sepharose that pre-coated by purified GST protein via GST antibody (control beads) or pre-coated by PAR via PAR antibody in G-PEM buffer, containing 20 μM paclitaxel, to form the reaction buffer. Purified PAR-binding domain of Spindly, Mcak, or Clip170 (Spb, Mpb, or Clpb, 20 nM) was added and incubated in the reaction buffer at room temperature for 10 min. A 5 μL aliquot of each reaction mix was mounted on a slide and sealed with a glass coverslip. The capture of microtubules by beads was observed under a confocal microscope at ×40/1.3 (Carl Zeiss 710).

Statistical analyses

All experiments were performed in triplicates unless indicated otherwise. Means and standard deviations were plotted. Student's *t* test was used for statistical analyses.

ACKNOWLEDGEMENTS

We are grateful to Dr. Bo Xiong for the insightful comments and suggestions on the manuscript. This work was supported by the grants from "Reproductive health and major birth defects prevention and control research" of Key Special Fund (2016YFC1000604), "Mechanism and clinical application of oocyte in vitro maturation" of Key Special Fund (2017YFC1001501), and the Foundation for Innovative Research Groups of the National Natural Science Foundation of China (81521002). M. L. is a member of Thousand Young Talents Program of China.

AUTHOR CONTRIBUTIONS

M.L. and J.Q. conceived and designed the experiments; B.X., L.Z., H.Z., Q.B., Y.F., X.Z., and X.L. performed the experiments; M.L., Y.Y., R.L., Q.-Y.S., and J.Q. wrote the manuscript.

ADDITIONAL INFORMATION

Supplementary information accompanies this paper at https://doi.org/10.1038/s41422-018-0009-7.

Competing interests: The authors declare no competing financial interests.

Publisher's note: Springer Nature remains neutral with regard to jurisdictional claims in published maps and institutional affiliations.

REFERENCES

1. Verlhac, M. H., Lefebvre, C., Guillaud, P., Rassinier, P. & Maro, B. Asymmetric division in mouse oocytes: with or without Mos. *Curr. Biol.* **10**, 1303–1306 (2000).
2. Li, L., Zheng, P. & Dean, J. Maternal control of early mouse development. *Development* **137**, 859–870 (2010).
3. Yi, K. et al. Dynamic maintenance of asymmetric meiotic spindle position through Arp2/3-complex-driven cytoplasmic streaming in mouse oocytes. *Nat. Cell Biol.* **13**, 1252–1258 (2011).
4. Chaigne, A., et al. A soft cortex is essential for asymmetric spindle positioning in mouse oocytes. *Nat. Cell Biol.* **15**, 958–966 (2013).
5. Schuh, M. & Ellenberg, J. A new model for asymmetric spindle positioning in mouse oocytes. *Curr. Biol.* **18**, 1986–1992 (2008).
6. Tripathi, A., Kumar, K. V. & Chaube, S. K. Meiotic cell cycle arrest in mammalian oocytes. *J. Cell Physiol.* **223**, 592–600 (2010).
7. Liang, C. G., Su, Y. Q., Fan, H. Y., Schatten, H. & Sun, Q. Y. Mechanisms regulating oocyte meiotic resumption: roles of mitogen-activated protein kinase. *Mol. Endocrinol.* **21**, 2037–2055 (2007).
8. Li, R. & Albertini, D. F. The road to maturation: somatic cell interaction and self-organization of the mammalian oocyte. *Nat. Rev. Mol. Cell. Biol.* **14**, 141–152 (2013).
9. Howe, K. & FitzHarris, G. Recent insights into spindle function in mammalian oocytes and early embryos. *Biol. Reprod.* **89**, 71 (2013).
10. Yi, K., Rubinstein, B. & Li, R. Symmetry breaking and polarity establishment during mouse oocyte maturation. *Philos. Trans. R. Soc. Lond. Ser. B* **368**, 20130002 (2013).
11. Fabritius, A. S., Ellefson, M. L. & McNally, F. J. Nuclear and spindle positioning during oocyte meiosis. *Curr. Opin. Cell Biol.* **23**, 78–84 (2011).
12. Szollosi, D., Calarco, P. & Donahue, R. P. Absence of centrioles in the first and second meiotic spindles of mouse oocytes. *J. Cell Sci.* **11**, 521–541 (1972).
13. Sathananthan, A. H. et al. From oogonia to mature oocytes: inactivation of the maternal centrosome in humans. *Microsc. Res. Technol.* **69**, 396–407 (2006).
14. Pearson, C. G. & Bloom, K. Dynamic microtubules lead the way for spindle positioning. *Nat. Rev. Mol. Cell. Biol.* **5**, 481–492 (2004).
15. Li, H., Guo, F., Rubinstein, B. & Li, R. Actin-driven chromosomal motility leads to symmetry breaking in mammalian meiotic oocytes. *Nat. Cell Biol.* **10**, 1301–1308 (2008).
16. Azoury, J. et al. Spindle positioning in mouse oocytes relies on a dynamic meshwork of actin filaments. *Curr. Biol.* **18**, 1514–1519 (2008).
17. Yi, K. et al. Sequential actin-based pushing forces drive meiosis I chromosome migration and symmetry breaking in oocytes. *J. Cell Biol.* **200**, 567–576 (2013).
18. Yi, K. & Li, R. Actin cytoskeleton in cell polarity and asymmetric division during mouse oocyte maturation. *Cytoskeleton* **69**, 727–737 (2012).
19. D'Amours, D., Desnoyers, S., D'Silva, I. & Poirier, G. G. Poly(ADP-ribosyl)ation reactions in the regulation of nuclear functions. *Biochem. J.* **342**(Part 2), 249–268 (1999).
20. Chambon, P., Weill, J. D. & Mandel, P. Nicotinamide mononucleotide activation of new DNA-dependent polyadenylic acid synthesizing nuclear enzyme. *Biochem. Biophys. Res. Commun.* **11**, 39–43 (1963).
21. Weill, J. D., Busch, S., Chambon, P. & Mandel, P. The effect of estradiol injections upon chicken liver nuclei ribonucleic acid polymerase. *Biochem. Biophys. Res. Commun.* **10**, 122–126 (1963).
22. Schreiber, V., Dantzer, F., Ame, J. C. & de Murcia, G. Poly(ADP-ribose): novel functions for an old molecule. *Nat. Rev. Mol. Cell. Biol.* **7**, 517–528 (2006).
23. Li, M. & Yu, X. Function of BRCA1 in the DNA damage response is mediated by ADP-ribosylation. *Cancer Cell.* **23**, 693–704 (2013).
24. Slade, D. et al. The structure and catalytic mechanism of a poly(ADP-ribose) glycohydrolase. *Nature* **477**, 616–620 (2011).
25. Miwa, M. & Sugimura, T. Splitting of the ribose-ribose linkage of poly(adenosine diphosphate-robose) by a calf thymus extract. *J. Biol. Chem.* **246**, 6362–6364 (1971).
26. Ahel, I., et al. Poly(ADP-ribose)-binding zinc finger motifs in DNA repair/checkpoint proteins. *Nature* **451**, 81–85 (2008).
27. Chang, P., Coughlin, M. & Mitchison, T. J. Tankyrase-1 polymerization of poly(ADP-ribose) is required for spindle structure and function. *Nat. Cell Biol.* **7**, 1133–1139 (2005).
28. Chang, P., Jacobson, M. K. & Mitchison, T. J. Poly(ADP-ribose) is required for spindle assembly and structure. *Nature* **432**, 645–649 (2004).
29. Thorslund, T., et al. Cooperation of the Cockayne syndrome group B protein and poly(ADP-ribose) polymerase 1 in the response to oxidative stress. *Mol. Cell. Biol.* **25**, 7625–7636 (2005).
30. Chaigne, A., et al. A narrow window of cortical tension guides asymmetric spindle positioning in the mouse oocyte. *Nat. Commun.* **6**, 6027 (2015).
31. Louvet, S., Aghion, J., Santa-Maria, A., Mangeat, P. & Maro, B. Ezrin becomes restricted to outer cells following asymmetrical division in the preimplantation mouse embryo. *Dev. Biol.* **177**, 568–579 (1996).
32. Ohi, R., Burbank, K., Liu, Q. & Mitchison, T. J. Nonredundant functions of Kinesin-13s during meiotic spindle assembly. *Curr. Biol.* **17**, 953–959 (2007).
33. Houghtaling, B. R., Yang, G., Matov, A., Danuser, G. & Kapoor, T. M. Op18 reveals the contribution of nonkinetochore microtubules to the dynamic organization of the vertebrate meiotic spindle. *Proc. Natl. Acad. Sci. USA* **106**, 15338–15343 (2009).
34. Akhmanova, A. & Steinmetz, M. O. Tracking the ends: a dynamic protein network controls the fate of microtubule tips. *Nat. Rev. Mol. Cell. Biol.* **9**, 309–322 (2008).
35. Burkel, B. M., von Dassow, G. & Bement, W. M. Versatile fluorescent probes for actin filaments based on the actin-binding domain of utrophin. *Cell. Motil. Cytoskelet.* **64**, 822–832 (2007).
36. Gueth-Hallonet, C., et al gamma-Tubulin is present in acentriolar MTOCs during early mouse development. *J. Cell. Sci.* **105**(Part 1), 157–166 (1993).
37. Chaigne, A., Terret, M. E. & Verlhac, M. H. Asymmetries and symmetries in the mouse oocyte and zygote. *Results Probl. Cell Differ.* **61**, 285–299 (2017).
38. Hiruma, Y., et al. Cell division cycle. Competition between MPS1 and microtubules at kinetochores regulates spindle checkpoint signaling. *Science* **348**, 1264–1267 (2015).
39. Procopio, M. G., et al. Combined CSL and p53 downregulation promotes cancer-associated fibroblast activation. *Nat. Cell Biol.* **17**, 1193–1204 (2015).
40. Kim, M. Y., Zhang, T. & Kraus, W. L. Poly(ADP-ribosyl)ation by PARP-1: "PAR-laying" NAD+ into a nuclear signal. *Genes Dev.* **19**, 1951–1967 (2005).

41. Ferreira, J. G., Pereira, A. L. & Maiato, H. Microtubule plus-end tracking proteins and their roles in cell division. *Int. Rev. Cell. Mol. Biol.* **309**, 59–140 (2014).
42. Akhmanova, A. & Steinmetz, M. O. Control of microtubule organization and dynamics: two ends in the limelight. *Nat. Rev. Mol. Cell. Biol.* **16**, 711–726 (2015).
43. Cooper, J. R., Wagenbach, M., Asbury, C. L. & Wordeman, L. Catalysis of the microtubule on-rate is the major parameter regulating the depolymerase activity of MCAK. *Nat. Struct. Mol. Biol.* **17**, 77–82 (2010).
44. Kumar, P., et al. Multisite phosphorylation disrupts arginine-glutamate salt bridge networks required for binding of cytoplasmic linker-associated protein 2 (CLASP2) to end-binding protein 1 (EB1). *J. Biol. Chem.* **287**, 17050–17064 (2012).
45. Mishima, M., et al. Structural basis for tubulin recognition by cytoplasmic linker protein 170 and its autoinhibition. *Proc. Natl. Acad. Sci. USA* **104**, 10346–10351 (2007).
46. Rieder, C. L. The structure of the cold-stable kinetochore fiber in metaphase PtK1 cells. *Chromosoma* **84**, 145–158 (1981).
47. Matthews, J. N. et al. The polymerization of actin: extent of polymerization under pressure, volume change of polymerization, and relaxation after temperature jumps. *J. Chem. Phys.* **123**, 074904 (2005).
48. Bean, G. J. & Amann, K. J. Polymerization properties of the *Thermotoga maritima* actin MreB: roles of temperature, nucleotides, and ions. *Biochemistry* **47**, 826–835 (2008).
49. Gibson, B. A. & Kraus, W. L. New insights into the molecular and cellular functions of poly(ADP-ribose) and PARPs. *Nat. Rev. Mol. Cell. Biol.* **13**, 411–424 (2012).
50. Su, X., et al. Phase separation of signaling molecules promotes T cell receptor signal transduction. *Science* **352**, 595–599 (2016).
51. Bergeron-Sandoval, L. P., Safaee, N. & Michnick, S. W. Mechanisms and consequences of macromolecular phase separation. *Cell* **165**, 1067–1079 (2016).
52. Hyman, A. A., Weber, C. A. & Julicher, F. Liquid-liquid phase separation in biology. *Annu. Rev. Cell Dev. Biol.* **30**, 39–58 (2014).
53. Siller, K. H. & Doe, C. Q. Spindle orientation during asymmetric cell division. *Nat. Cell Biol.* **11**, 365–374 (2009).
54. Griffis, E. R., Stuurman, N. & Vale, R. D. Spindly, a novel protein essential for silencing the spindle assembly checkpoint, recruits dynein to the kinetochore. *J. Cell Biol.* **177**, 1005–1015 (2007).
55. Ovechkina, Y., Wagenbach, M. & Wordeman, L. K-loop insertion restores microtubule depolymerizing activity of a "neckless" MCAK mutant. *J. Cell Biol.* **159**, 557–562 (2002).